

# Formation of Contaminant Droplets on Surfaces

15 December 2006

Prepared by

K. T. LUEY and D. J. COLEMAN  
Space Materials Laboratory  
Laboratory Operations

Prepared for

SPACE AND MISSILE SYSTEMS CENTER  
AIR FORCE SPACE COMMAND  
483 N. Aviation Blvd.  
El Segundo, CA 90245-2808

Engineering and Technology Group

This report was submitted by The Aerospace Corporation, El Segundo, CA 90245-4691, under Contract No. FA8802-04-C-0001 with the Space and Missile Systems Center, 483 N. Aviation Blvd., El Segundo, CA 90245. It was reviewed and approved for The Aerospace Corporation by G. F. Hawkins Principal Director, Space Materials Laboratory; and D. C. Marvin, Principal Director, Office of Research & Technology Applications. Michael Zambrana was the project officer for the Mission-Oriented Investigation and Experimentation (MOIE) program.

This report has been reviewed by the Public Affairs Office (PAS) and is releasable to the National Technical Information Service (NTIS). At NTIS, it will be available to the general public, including foreign nationals.

This technical report has been reviewed and is approved for publication. Publication of this report does not constitute Air Force approval of the report's findings or conclusions. It is published only for the exchange and stimulation of ideas.

A handwritten signature in black ink, appearing to read "Michael Zambrana", written over a horizontal line.

Michael Zambrana  
SMC/EA

# REPORT DOCUMENTATION PAGE

*Form Approved*  
OMB No. 0704-0188

Public reporting burden for this collection of information is estimated to average 1 hour per response, including the time for reviewing instructions, searching existing data sources, gathering and maintaining the data needed, and completing and reviewing this collection of information. Send comments regarding this burden estimate or any other aspect of this collection of information, including suggestions for reducing this burden to Department of Defense, Washington Headquarters Services, Directorate for Information Operations and Reports (0704-0188), 1215 Jefferson Davis Highway, Suite 1204, Arlington, VA 22202-4302. Respondents should be aware that notwithstanding any other provision of law, no person shall be subject to any penalty for failing to comply with a collection of information if it does not display a currently valid OMB control number. **PLEASE DO NOT RETURN YOUR FORM TO THE ABOVE ADDRESS.**

<b>1. REPORT DATE (DD-MM-YYYY)</b> 15-12-2006		<b>2. REPORT TYPE</b>		<b>3. DATES COVERED (From - To)</b>	
<b>4. TITLE AND SUBTITLE</b>  Formation of Contaminant Droplets on Surfaces				<b>5a. CONTRACT NUMBER</b> FA8802-04-C-0001	
				<b>5b. GRANT NUMBER</b>	
				<b>5c. PROGRAM ELEMENT NUMBER</b>	
<b>6. AUTHOR(S)</b>  K. T. Luey and D. J. Coleman				<b>5d. PROJECT NUMBER</b>	
				<b>5e. TASK NUMBER</b>	
				<b>5f. WORK UNIT NUMBER</b>	
<b>7. PERFORMING ORGANIZATION NAME(S) AND ADDRESS(ES)</b>  The Aerospace Corporation Laboratory Operations El Segundo, CA 90245-4691				<b>8. PERFORMING ORGANIZATION REPORT NUMBER</b>  TR-2006(8565)-10	
<b>9. SPONSORING / MONITORING AGENCY NAME(S) AND ADDRESS(ES)</b> Space and Missile Systems Center Air Force Space Command 483 N. Aviation Blvd. El Segundo, CA 90245				<b>10. SPONSOR/MONITOR'S ACRONYM(S)</b> SMC	
<b>12. DISTRIBUTION/AVAILABILITY STATEMENT</b>  Approved for public release; distribution unlimited.				<b>11. SPONSOR/MONITOR'S REPORT NUMBER(S)</b>	
				<b>13. SUPPLEMENTARY NOTES</b>	
<b>14. ABSTRACT</b>  The effects of molecular film contamination on optical systems depend strongly on the film uniformity and thickness. Molecular films of uniform thickness are responsible for light transmission losses through absorption. For example, a partially darkened film of dioctyl phthalate 100 Å thick may cause losses of about 2% in the visible spectrum. However, Ternet, et al, Villahermosa, et al, and others have shown that scattering from droplets or "puddles" can cause transmission losses of 30%. In this report, we examine properties of the contaminant and surface that drive the formation of smooth films and droplets. It is shown that surfaces play a strong and sometimes dominant role in controlling film or droplet formation. DC 704, a high-purity, siloxane liquid, is shown to assume both droplet and smooth film character depending on the surface.					
<b>15. SUBJECT TERMS</b>  Molecular contamination, Contaminant films, Droplets, Surface tension					
<b>16. SECURITY CLASSIFICATION OF:</b>			<b>17. LIMITATION OF ABSTRACT</b>	<b>18. NUMBER OF PAGES</b>	<b>19a. NAME OF RESPONSIBLE PERSON</b> Ken Luey
<b>a. REPORT</b> UNCLASSIFIED	<b>b. ABSTRACT</b> UNCLASSIFIED	<b>c. THIS PAGE</b> UNCLASSIFIED			<b>19b. TELEPHONE NUMBER (include area code)</b> (310)336-5499

## **Acknowledgements**

The authors gratefully acknowledge skillful microscopic analysis by Ms. Judy Ying and insightful technical discussions with Dr. G. K. Ternet and Ms. Sonia Esparza.

This work was supported under The Aerospace Corporation's Mission Oriented Investigation and Experimentation program, funded by the U.S. Air Force Space and Missile Systems Center under Contract No. FA8802-04-C-0001.

## Contents

1. Introduction .....	1
2. Background.....	3
3. Experimental Survey.....	7
3.1 Initial E595 Evaluation.....	7
3.2 Testing of Other Materials.....	11
4. Summary .....	15
References.....	17

## Figures

1. Transmitted light intensity as a function of wavelength and film thickness, $I(\lambda, \tau)$ , for DC 704 vacuum deposited in the presence of VUV radiation. ....	4
2. Siloxane film deposited and darkened by proton radiation on transparent glass substrates. ....	4
3. Vacuum deposited droplets of DC 704 on fused silica.....	6
4. Optical photomicrograph of contaminant droplets on an optical window. ....	6
5. Four collector samples exposed to DC 704 source in E595 apparatus.....	7
6. DC 704 deposited on (a) fused silica and (b) vapor-deposited gold.....	8
7. Optical photomicrographs of DC 704 on (a) fused silica and (b) vapor-deposited gold.....	9
8. Vacuum deposition of DC 704 – DC 200 mixture in E595 apparatus .....	9
9. DC 704 DC 200 mixture on vapor-deposited aluminum.....	10
10. Properties of DC 704 - DC 200 mixture.....	10
11. DC 704 vacuum deposited on copper. ....	12

12. DC 704 deposited on (a) platinum and (b) tungsten.....	12
13. DC 704 deposited on (a) MgF <sub>2</sub> coating on fused silica cover glass (31 μg) and (b) Kapton (polyamide) film (37 μg).....	13
14. 30 μg of DC 704 deposited on vapor-deposited gold.....	13
15. 100 μg of DC 704 deposited on vapor-deposited gold at two magnifications.....	14
16. 100 μg of DC 704 deposited on (a) vapor-deposited platinum and (b) vapor-deposited chromium.....	14

### Table

1. Surface Energies of Test Materials.....	11
--	----

## 1. Introduction

For many years, contamination effects due to molecular films have been measured and calculated assuming a thin, uniform structure. This assumption is likely a good one for films outgassed from spacecraft nonmetallic materials and deposited in strong radiation environments such as geosynchronous orbit. More recently, interest has increased in molecular films that deposit as arrays of droplets, islands, or “puddles.” Anecdotal evidence suggests that this configuration might occur in environments with no vacuum ultraviolet (VUV) radiation. The key question, therefore, is “Does a molecular film deposit as a smooth, uniform film? Or as an array of droplets?” The answer is important because the difference in optical transmission loss can be very large between the two cases. In this report, factors affecting the deposition of molecular films and droplets are examined.

## 2. Background

For many decades, contamination affecting spacecraft performance and lifetime fell into two categories:

- Microscopic dust and manufacturing debris; and
- Molecular films condensed from outgassing, nonmetallic materials.

Dust and debris caused optical obscuration and were viewed as distinct entities having properties that did not evolve with time or temperature, although particle redistribution during launch and ascent was of significant concern.

In contrast, condensed molecular films from outgassing materials have properties that depend on source temperature, receiver temperature, surface adsorption energy, chemical reactivity, and photochemical reactivity with VUV and high-energy particulate radiation.

During 1970–2000, vigorous laboratory research,<sup>1–5</sup> together with on-orbit space system measurements,<sup>6,7</sup> concluded that molecular films deposit for long times, with some flight data suggesting the process can last at least eight years. Space radiation facilitates the film growth via photochemical fixing and also darkens the film because it provides the energy for cross-linking polymerization. The spectral transmission of such a film (DC704, a high-purity siloxane pump oil used as a silicone outgassing analog) is shown in Figure 1.

Figure 1 plots the ratio:

$$I(\lambda, \tau)/I(\lambda, \tau=0) \quad (1)$$

where  $\lambda$  is the wavelength of light,  $\tau$  is the film thickness, and  $I(\lambda, \tau)$  is given by Beer's Law:

$$I(\lambda, \tau) = A(\lambda, \tau=0) \exp[-\alpha(\lambda, \tau)\tau]. \quad (2)$$

$\alpha(\lambda, \tau)$  is the absorption coefficient as a function of wavelength and film thickness.

Equation (1) and Figure 1 describe a largely smooth, uniform film that eventually takes on a yellow-brown tint, but is still transparent. It looks similar to a colored glass. A film of siloxane pump oil deposited and darkened by proton irradiation is shown in Figure 2.



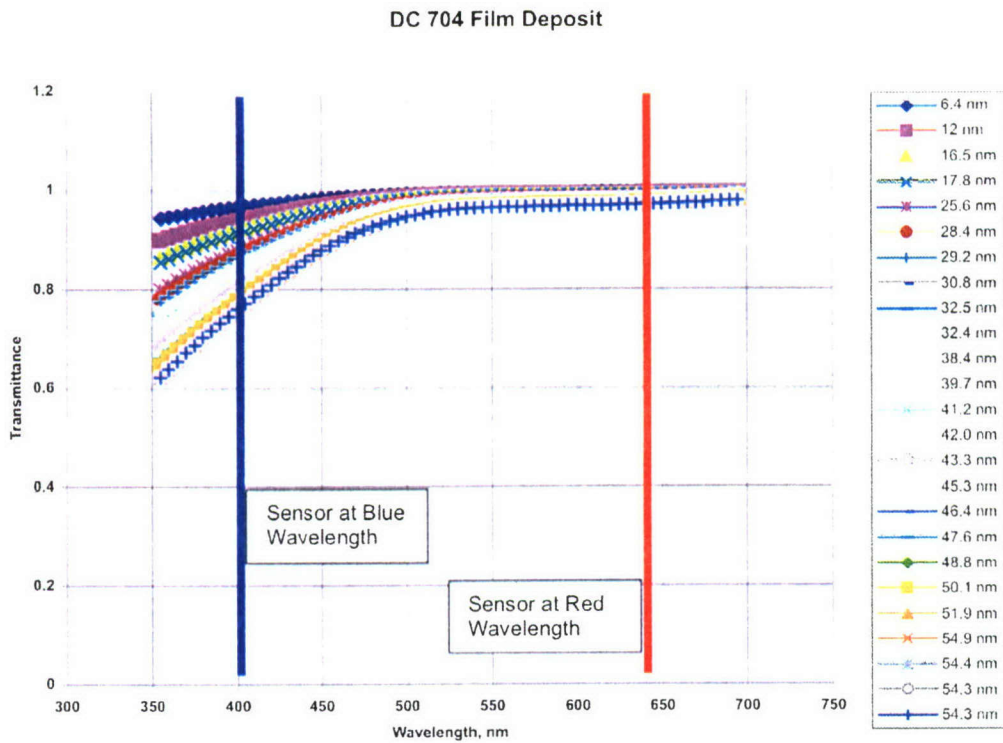


Figure 1. Transmitted light intensity as a function of wavelength and film thickness,  $I(\lambda, \tau)$ , for DC 704 vacuum deposited in the presence of VUV radiation.

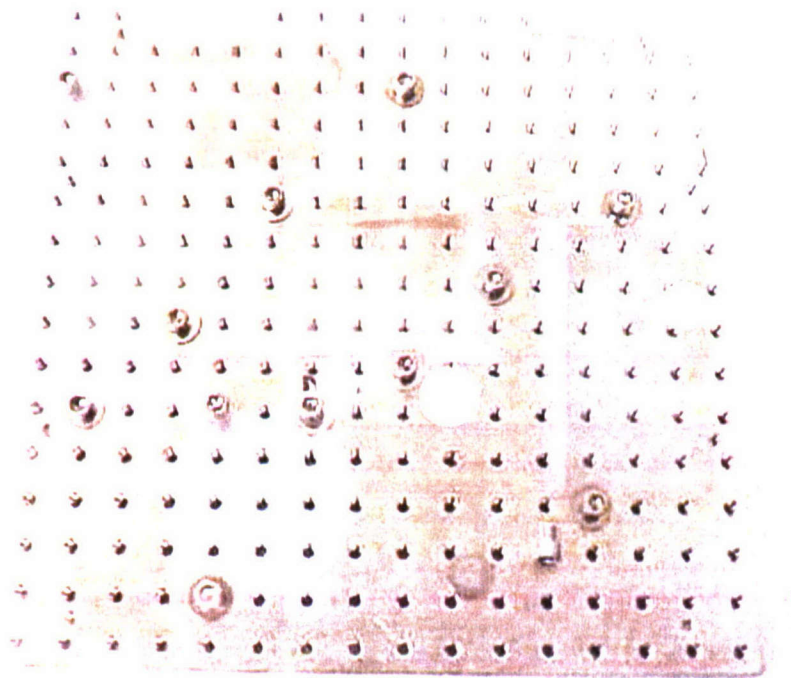


Figure 2. Siloxane film deposited and darkened by proton radiation on transparent glass substrates.

Today, there is much greater interest in non-uniform molecular films. These films consist of droplets or patchy islands. These droplets appear mostly to have contact angles  $\approx 10^\circ$  and are therefore flat rather than spherical. The films have a foggy or hazy appearance, and one can usually not see through them. These are manifestations of scattering effects. Scattering effects, including haze and opacity, were observed for vacuum-deposited 10-nonadecanone, dodeca-hydro-triphenylene (DTP), and bi-benzyl. But these scattering films were not studied because of the need for more sophisticated equipment. More recently, the bi-directional reflectance distribution function (BRDF) of DTP and non-irradiated films of DC704 and dioctyl phthalate have been measured by Ternet, Barrie, and Olson.<sup>8</sup>

Previously, Krone-Schmidt and Loveridge<sup>9</sup> measured the BRDF of the fuel MMH-nitrate on bare Be mirrors. With the Be mirror surface at temperatures between 200K and 250K, they found that MMH deposited at slow to moderate rates formed films with negligible scatter. However, MMH deposited at higher rates formed diffusely scattering films.

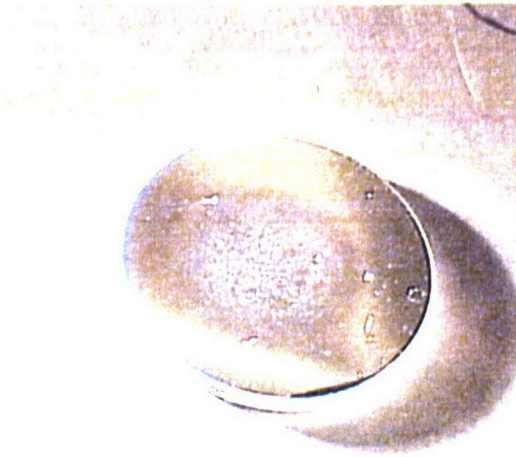
During 1990–1995, Seiber, Bryson, Bertrand, and Wood<sup>10</sup> performed cryogenic BRDF measurements at 10.6 and 0.63  $\mu\text{m}$  on contaminated mirrors. The mirrors were exposed to air,  $\text{N}_2$ ,  $\text{O}_2$ , CO, Ar, and  $\text{H}_2\text{O}$  at temperatures near 18K. In addition, mirrors contaminated by polycyanurate resin, NuSil CV2500 silicone, solithane polyurethane, and RTV 560 silicone were measured. Many of the films became diffuse scatterers as the thickness increased.  $\text{H}_2\text{O}$  films showed large increases in scatter when the film shattered or fractured at temperatures near 20K. These investigators found only small differences in scatter caused by thin films of outgassed silicones and resins. More complicated behavior was observed for solithane in which scatter increased with film thickness, but then decreased suddenly.

Two events, among many others, have stimulated new interest in the scattering properties of molecular films. First is the observation by Villahermosa and Coleman<sup>11</sup> that vacuum-deposited DC 704 deposits as an array of thin droplets on a vapor-deposited aluminum mirror in the absence of VUV radiation, as shown in Figure 3(a). Figure 3(a) shows a deposited sample in a vacuum chamber just prior to UV irradiation and appears as a hazy, opaque film, unlike those shown in Figure 2. Figure 3(b) shows the same sample following irradiation from a deuterium VUV lamp for about 10 hours. While the resulting film is not perfectly uniform, the droplets have converted to a film spread out over the surface. The VUV has reduced the surface tension of the aluminum/silicone interface.

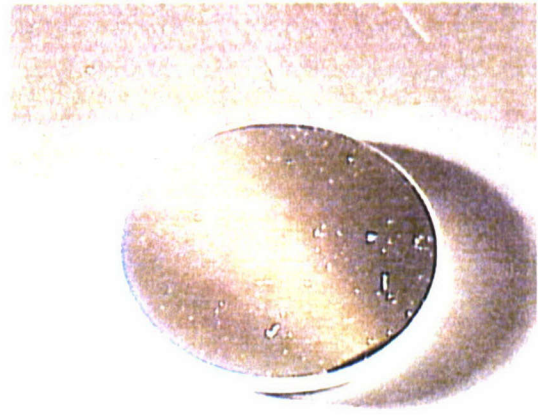
Second is the recent investigation and resolution of an anomaly involving the large loss of optical light transmission in the visible wavelengths for an optical system. During a subsequent vacuum test, an identical system was shown to develop nearly the same amount of loss in less than one year. Following removal from the vacuum, an interior optical window was found to be contaminated with a condensed film consisting of droplets, as shown in Figure 4.

This window is located deep within the instrument behind several other optical components that would absorb VUV radiation. The lack of VUV in the ground test is likely an accurate representation of the conditions experienced in space.

These incidents and observations further emphasize the need for a deeper understanding of how molecular film contaminants form on various surfaces.



(a)



(b)

Figure 3. Vacuum deposited droplets of DC 704 on fused silica. (a) Before irradiation by VUV. (b) Following irradiation.

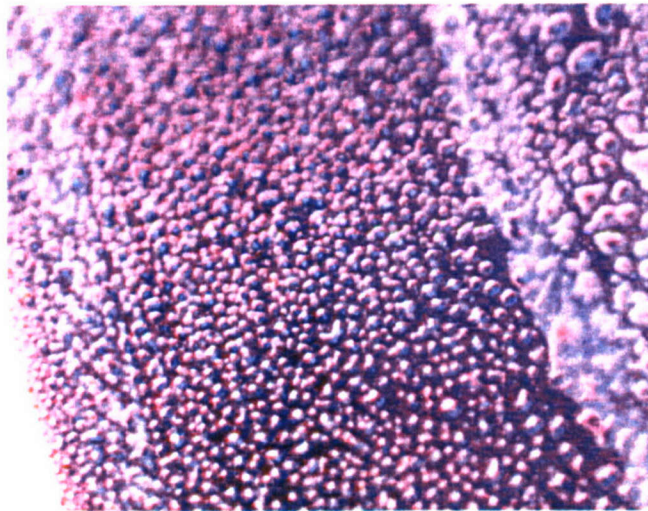


Figure 4. Optical photomicrograph of contaminant droplets on an optical window.

### 3. Experimental Survey

The fundamental principles governing the formation of liquid droplets and films have been studied and documented beginning in the early 19<sup>th</sup> century in work by Rayleigh and Young. In the study of ideal systems, three types of forces are in play: (1) the force between surface and liquid; (2) the force between liquid and atmosphere; and (3) the force between atmosphere and surface. Analysis of these systems often involves surface tension, capillarity, contact angles, and wetting. At present, these approaches have limited usefulness in predicting how contaminant films will behave on real surfaces since reliable data are not available for most real, engineered surfaces and contaminants. Additionally, the variety of droplet shapes and sizes in Figure 4 suggests that a mixture of contaminants is likely present, which is probably the realistic situation. In this effort, therefore, simple studies were deemed necessary to examine relationships between typical contaminant analogs and optical surfaces. Contaminants were first deposited on optical flats using an ASTM E595 apparatus. This method was fast and provided easily interpreted results. But the deposition rates were often unrealistically high. A second set of studies was performed using a temperature-controlled effusion cell and quartz-crystal microbalance. The experimental arrangement for that work was described in Reference 2.

#### 3.1 Initial E595 Evaluation

Figure 5 shows a set of collector samples exposed to vacuum vapor of DC 704 in an E595 apparatus. The collector set consists of: (1) polished silicon; (2) fused silica, (3) vapor-deposited aluminum on

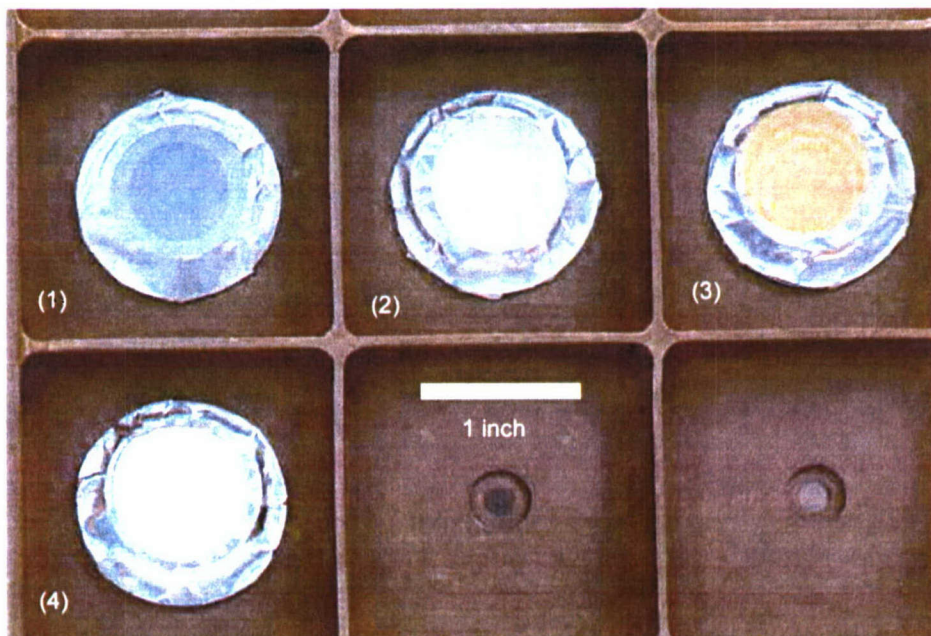


Figure 5. Four collector samples exposed to DC 704 source in E595 apparatus. (1) polished silicon; (2) fused silica; (3) vapor-deposited gold; (4) vapor-deposited aluminum.

fused silica; and (4) vapor-deposited gold on fused silica. The deposited masses of DC 704 ranged between 30 and 40  $\mu\text{g}$  and were deposited over a period of two hours with the source boat at  $45^\circ\text{C}$ .

Note that  $1 \mu\text{g}/\text{cm}^2$  is traditionally thought of as a thick, continuous film about  $100 \text{ \AA}$  thick. Figure 5 shows that DC 704 deposits differently on each collector and not as a continuous film of well-defined thickness, except in one case. Figure 6 shows higher magnification images of the fused silica (2) and vapor-deposited gold (3) samples. Figure 6(a) shows that the DC 704 deposits as an array of droplets. The array extends over a circular area about  $\frac{1}{2}$  in. in diameter. This area is characteristic of the distance between the source and collector in the E595 test chamber. Figure 6(b) shows that the very same DC 704, deposited during the same vacuum cycle, for the same time, and at the same temperature, forms on the gold surface as a film. The film is not smooth or uniform, but clearly extends over a greater area of the gold collector and displays refractive features. The differences in the film configuration are solely an effect of the collector material surface properties, such as the surface tension. There are no other differences between Figure 6(a) and 6(b).

Figure 7 shows optical photomicrographs of the samples shown in Figure 6. As shown previously, DC 704 forms on fused silica as droplets that have contact angles of about  $12^\circ$ , so they resemble relatively flat “puddles” instead of drops, as shown in Figure 7(a). Figure 7(b) shows that DC 704 flows on the gold surface, but tends to nucleate around film defects (possibly pinholes) and surface dust particles.

A simple interpretation of surface energies is consistent with these observations. References give the surface energy of gold as  $1400 \text{ ergs}/\text{cm}^2$  where the surface energy is defined as the difference between the bonding of an atom or molecule in bulk and its bonding state at a surface.<sup>11</sup> Similarly, the surface energy may be thought of as the energy needed to bring one unit from the bulk to the surface.

For ideal systems, the surface tension is often thought to be large for high-purity materials. More vacuum depositions were performed in the E595 apparatus using a mixture of DC 704 and DC 200 poly-dimethyl siloxane. While DC 704 is made up of tetra-methyl, tetra-phenyl trisiloxane, DC 200 contains linear siloxanes of many lengths. Initial results from that vacuum run are shown in Figure 8. The deposited masses were high, ranging between 90 and  $100 \mu\text{g}$ .

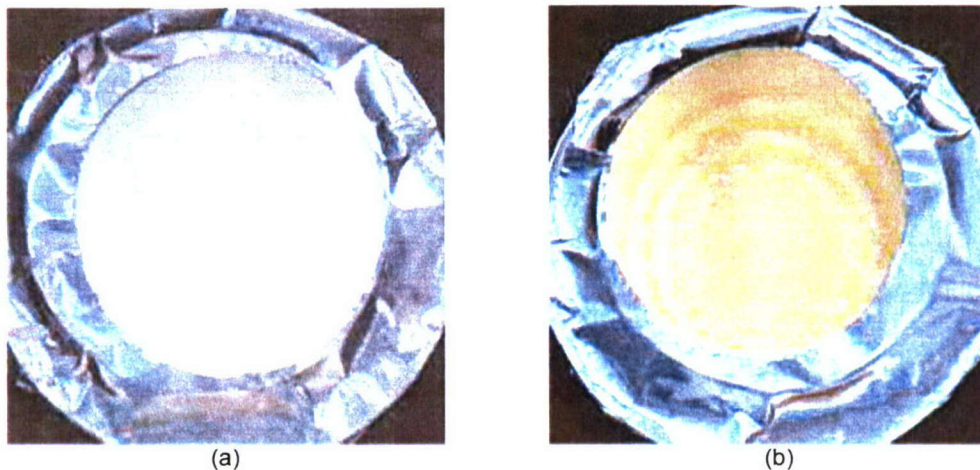


Figure 6. DC 704 deposited on (a) fused silica and (b) vapor-deposited gold.

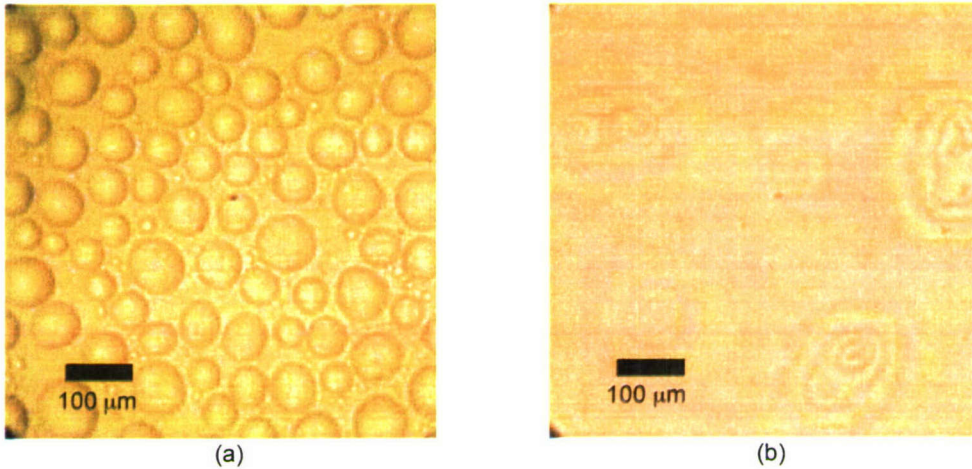


Figure 7. Optical photomicrographs of DC 704 on (a) fused silica and (b) vapor-deposited gold.

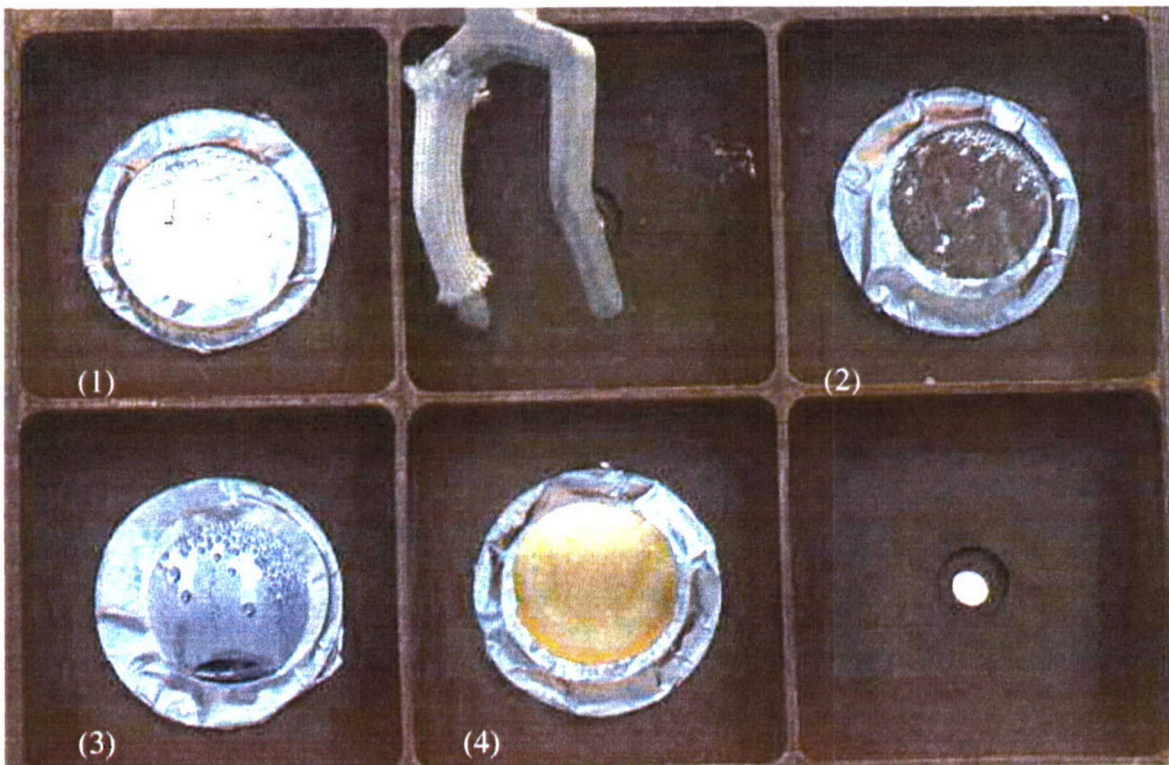


Figure 8. Vacuum deposition of DC 704 – DC 200 mixture in E595 apparatus. The collectors are: (1) polished silicon; (2) fused silica; (3) vapor-deposited aluminum; and (4) vapor-deposited gold.

The deposit on gold looks largely the same as in Figure 6, appearing as a refractive film spread out over much of the collector surface. The aluminum, silicon, and fused silica surfaces obviously look radically different. Large droplets appear to have formed with enough mass such that gravity has caused dripping. Collector (3) of vapor-deposited aluminum is of particular interest and is shown at

higher magnification in Figure 9. This sample displays many film and droplet characteristics, including segregated droplets of multiple sizes, and with varying contact angles, as well as some refractive regions in which film character exists.

For large masses of silicone deposit, Figure 10(a) shows that the mixture eventually coalesces into one uniform film. The film can then flow freely on the gold surface. Figure 10(b) shows that the silicones stay in their droplet form and do not flow except when held in a vertical position, as shown in Figure 8.

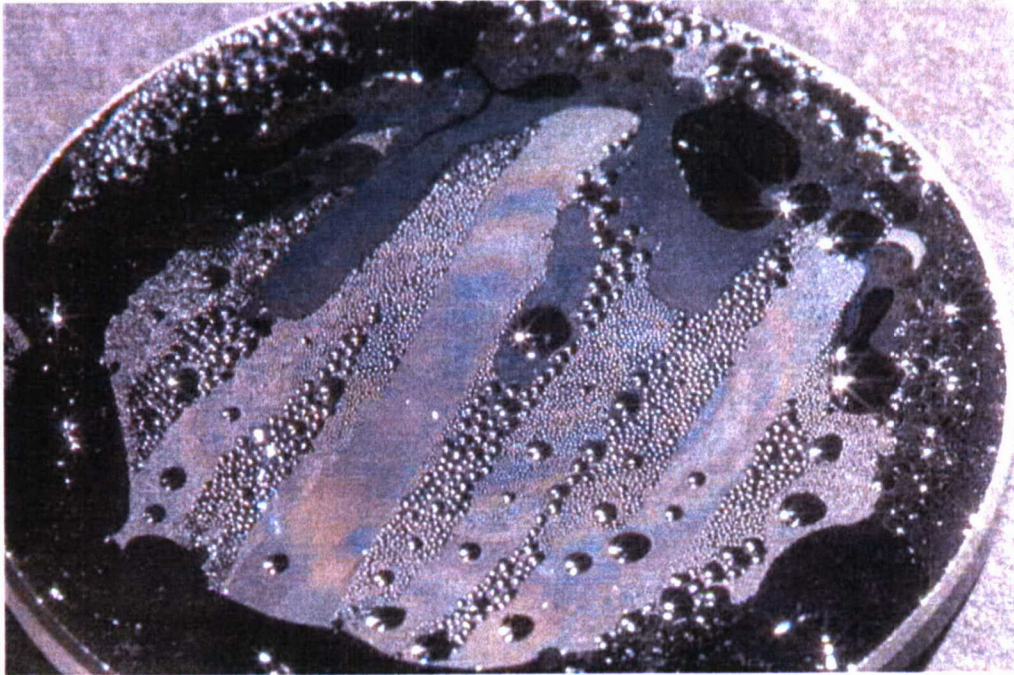


Figure 9. DC 704 DC 200 mixture on vapor-deposited aluminum.

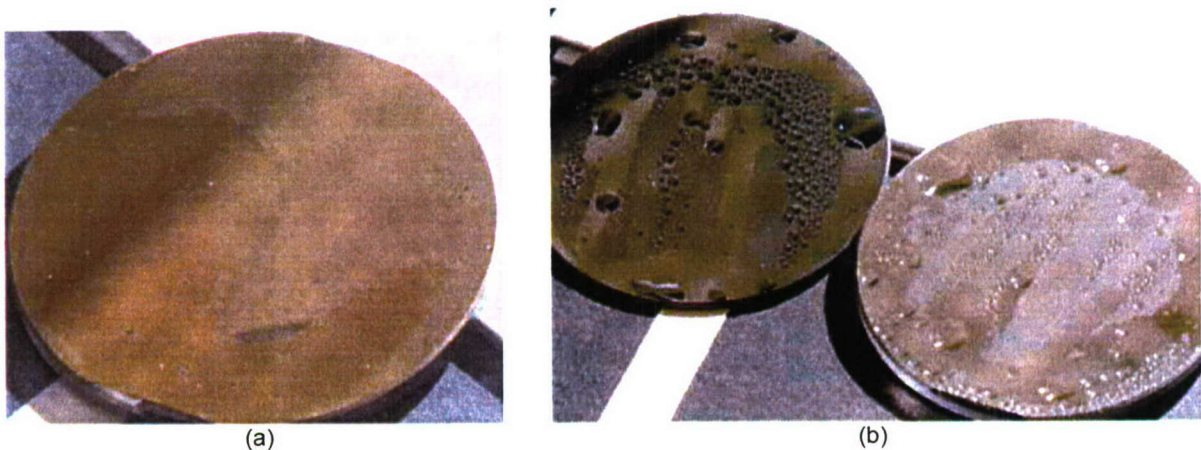


Figure 10. Properties of DC 704 - DC 200 mixture. (a) Silicone oil mixture coalesces into continuous film and flows on gold surface. (b) Silicone oil retains droplet shape on aluminum and silicon.

The results from this initial test suggest that the question of film or droplet formation has a complex answer. First, observations from the deposition of pure DC 704 show that the surface alone plays a significant role and that gold could be an important special case. Second, mixtures of materials have significantly different properties on the same surfaces. These initial tests suggest that simple “rules of thumb” are likely not possible for more realistic spaceflight situations where many materials and surfaces and various temperatures interact. Additionally, the simple interpretation of  $1 \mu\text{g}/\text{cm}^2$  being equivalent to a  $100 \text{ \AA}$  thick film is likely incorrect in many cases.

### 3.2 Testing of Other Materials

The previous section described the vacuum deposition of a silicone oil onto gold and various silicon-based substrates. A significant difference in the formation of films and droplets was found to depend on the substrate material. In this section, DC 704 is again vacuum deposited using an E595 test chamber, but onto a variety of other materials. These materials were selected initially for their tabulated surface energies or for their wide application in space systems. All of the samples shown in this section were deposited together in one vacuum run.

The tabulated surface energies for gold, copper, platinum, and tungsten are summarized in Table 1.<sup>12</sup> The melting point is given to indicate the purity of material.

Pure silicon is reported to have a surface energy of  $730 \text{ ergs}/\text{cm}^2$ , with values ranging as high as  $1440 \text{ ergs}/\text{cm}^2$  with bulk impurities. Values for the surface oxide or  $\text{SiO}_x$  have not been found, so various types of silicon optical surfaces are not included in Table 1.

A set of samples was selected for evaluation based on tabulated surface energies. The set consisted of vapor-deposited gold, and solid samples of copper, platinum, and tungsten. All samples were run in a single vacuum run in the E595 test chamber. The deposited masses of DC 704 ranged between  $30$  and  $40 \mu\text{g}$  to be near the deposition conditions of Ternet, et al.<sup>2</sup>

Table 1 indicates that copper has a surface energy comparable to gold. Figure 11 shows optical micrographs of DC 704 deposited on copper. The mass of DC 704 deposited was  $40 \mu\text{g}$ .

Films or droplets are not readily apparent due to the large amount of polishing marks and scratches.

Figure 12 shows deposition of DC 704 on platinum and tungsten, respectively.

Table 1. Surface Energies of Test Materials

Material	Surface Energy (ergs/cm <sup>2</sup> )	Melting Point (°C)
Gold	1140	1063
Copper	1300	1083
Platinum	1800	1773
Chromium	1590	1950
Tungsten	2400	3410



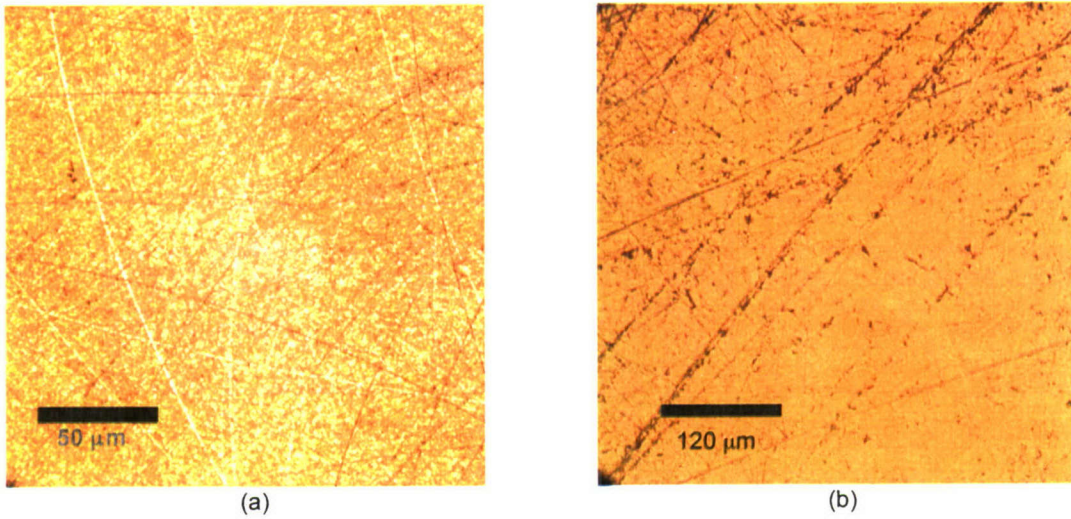


Figure 11. DC 704 vacuum deposited on copper.

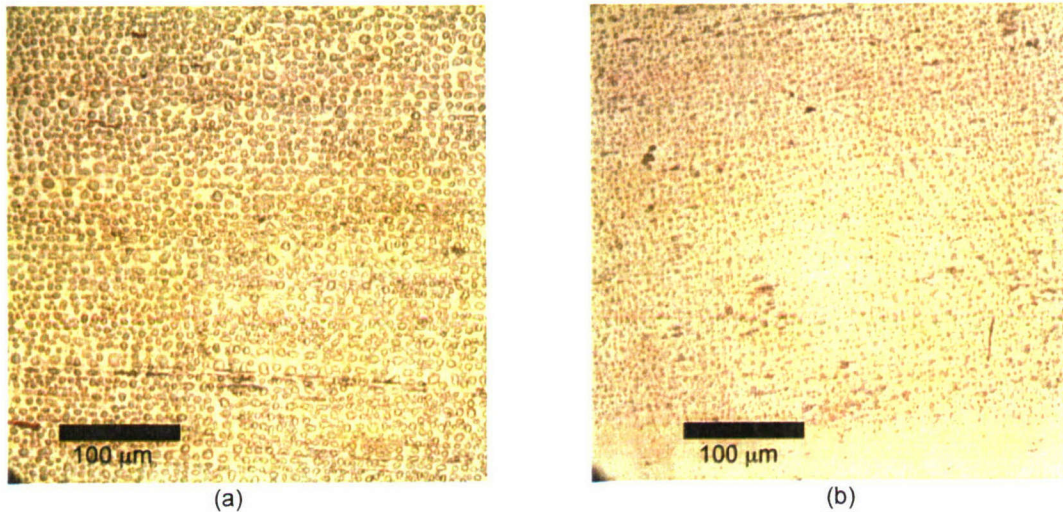


Figure 12. DC 704 deposited on (a) platinum and (b) tungsten.

The droplets formed are of differing size and density. Though their tabulated surface energies are not the same, both energies are significantly higher than gold.

Figure 13 shows the deposition of DC 704 on MgF<sub>1</sub> antireflection coating over fused-silica cover glass and on Kapton. Note that the droplet size varies significantly despite the same deposition rates and similar masses deposited. It is not known why droplets appear to form along crossed linear features on the MgF<sub>1</sub>, but is likely related to a scratch or other surface defect that affects the surface energy locally.

These results suggest that the DC 704 film first deposits on vapor-deposited gold as droplets and then coalesces into a film as the deposited mass accumulates.

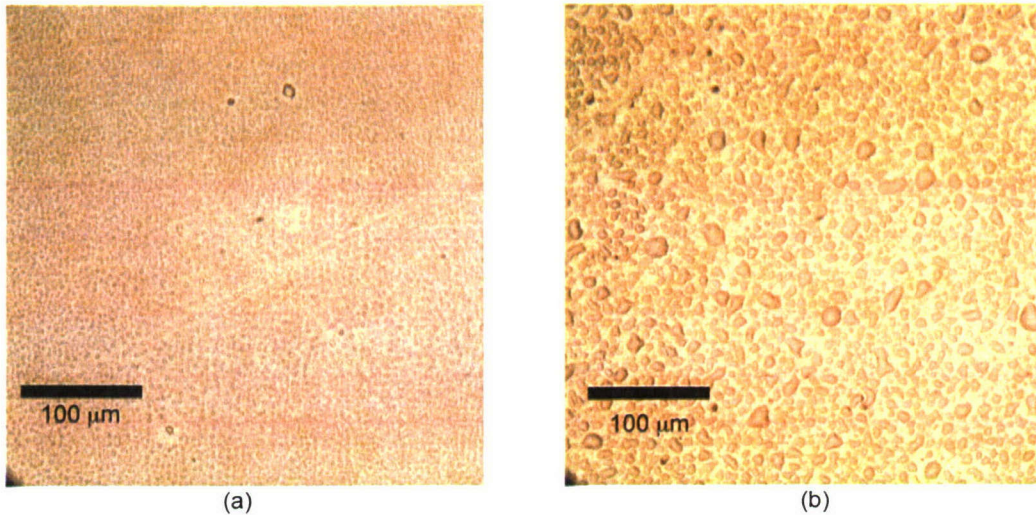


Figure 13. DC 704 deposited on (a) MgFl coating on fused silica cover glass (31  $\mu\text{g}$ ) and (b) Kapton (polyamide) film (37  $\mu\text{g}$ ).

Figure 14 shows that DC 704 droplets will form even on vapor-deposited gold surfaces if the deposition mass is small, about 30  $\mu\text{g}$ .

To assess this model, very large masses of DC 704, about 100  $\mu\text{g}$ , were vacuum deposited on gold, platinum, and chromium, where all the metal substrate films were vapor-deposited. DC 704 was deposited at the same rate, but for a longer time. The vapor-deposited gold sample is shown in Figure 15.

Note that the film appears to nucleate around surface defects or particles. Nucleation phenomena are more apparent on the vapor-deposited platinum and chromium samples shown in Figure 16.

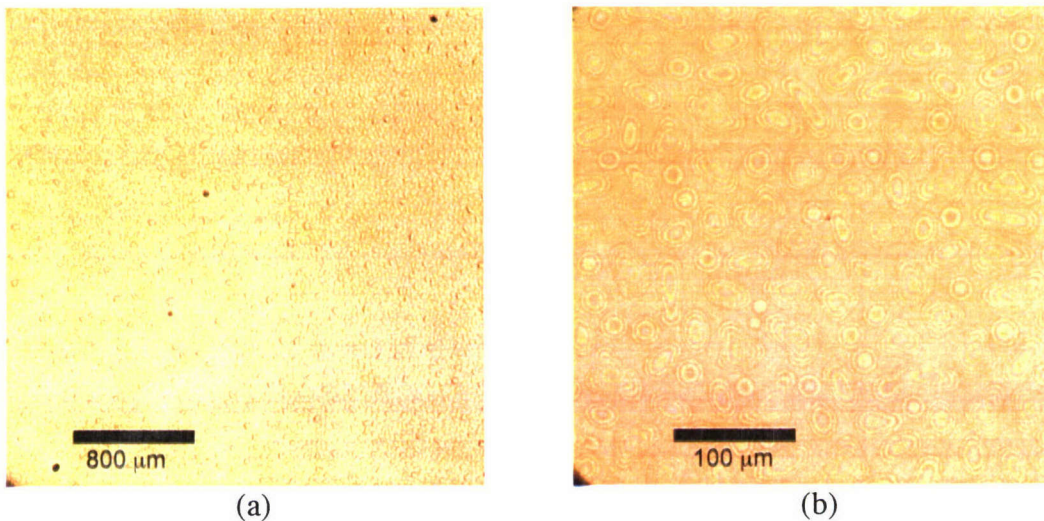


Figure 14. 30  $\mu\text{g}$  of DC 704 deposited on vapor-deposited gold.

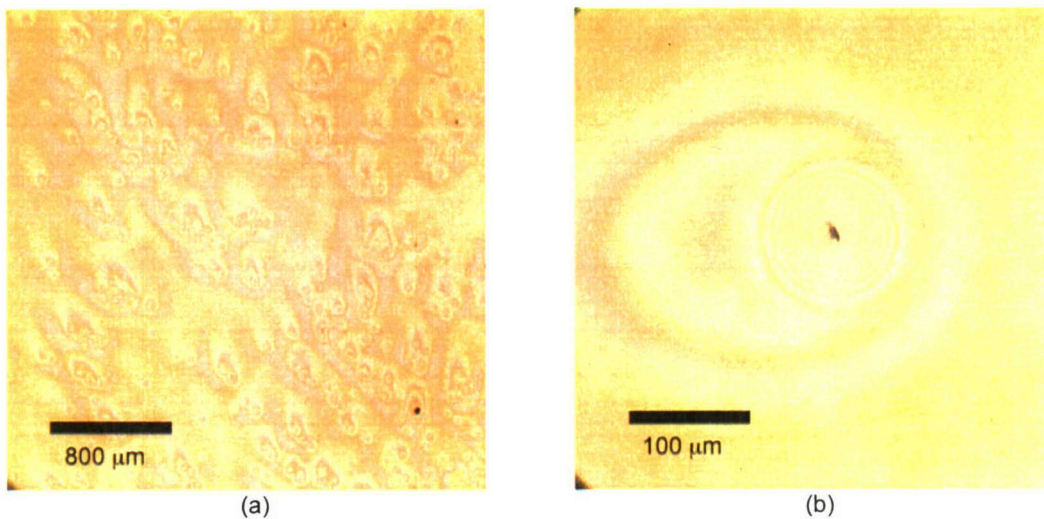


Figure 15. 100 μg of DC 704 deposited on vapor-deposited gold at two magnifications.

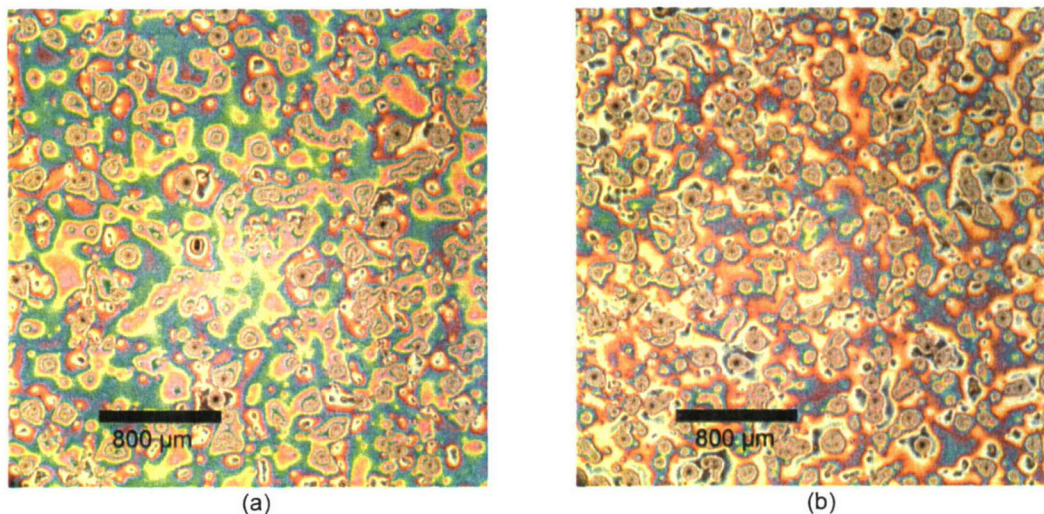


Figure 16. 100 μg of DC 704 deposited on (a) vapor-deposited platinum and (b) vapor-deposited chromium.

In these micrographs, there is a significant mixture of distributed film and nucleation of film around surface particles and defects. Platinum and chromium vapor depositions were performed in a separate chamber. SEM evaluation of the Pt and Cr substrates prior to DC 704 deposition show a higher than desired density of surface dirt particles. However, this test suggests that surface particulate contamination is another driver toward the formation of droplets or non-uniform films.

## 4. Summary

This study has attempted to determine major factors in the formation of contaminant droplets on ideal surfaces and applied spacecraft materials. The objective was to identify simple “rules of thumb” to predict film or droplet formation.

Observations following controlled depositions on selected materials suggest that many factors affect film growth. In ideal systems, surface energies could be important drivers, with metals such as gold defining a lower limit for smooth film formation. However, real materials contain surface scratches, polishing, and working that can cause large variations in the tabulated surface energy, thus promoting the formation of droplets. Other spacecraft materials that appear to promote droplet formation include engineered, multilayered antireflection coatings, silicon oxides ( $\text{SiO}_2$ ,  $\text{SiO}_x$ , etc.), and thermal control polymers with and without ESD coatings. These manufactured materials are likely to have high surface energies due to their complex bonding and manufactured structure. Additionally, the presence of surface particles appears to favor the formation of droplets or film discontinuities.

Two factors appear to favor the formation of films. First, large deposition masses on gold appear to form films if the surface is clean. Mixtures, as would be likely to occur in real applications, seem to have a better chance of spreading as films on gold. Future work will address the role of VUV radiation on enhancing the wettability of contaminant films on surfaces with high energies.

At present, simple “rules of thumb” are not possible, but engineering tests, such as more detailed microscopic examination of collected volatile condensable material from ASTM E595 tests, could prove useful.

## References

1. G. S. Arnold and K. T. Luey, "Photochemically deposited contaminant film effects," in *Optical Systems Contamination V and Stray Light and System Optimization*, Proceedings of SPIE, Vol. 2864, 5–7 August 1996, Denver CO, pp. 269-285.
2. T. B. Stewart, G. S. Arnold, D. F. Hall, D. C. Marvin, W. C. Hwang, and R. D. Chandler, "Photochemical Spacecraft Self Contamination: Laboratory Results and Systems Impacts," *J. Spacecraft*, **26**, pp. 358–366 (1989).
3. T. B. Stewart, G. S. Arnold, D. F. Hall, and H. D. Marten, "Absolute Rates of Vacuum Ultraviolet Photochemical Deposition of Organic Films," *J. Phys. Chem.*, **93**, 2392 (1989).
4. G. S. Arnold, R. C. Young Owl, and D. F. Hall, "Optical Effects of Photochemically Deposited Contaminant Films," in *Optical System Contamination: Effects, Measurement, and Control*, Proceedings of the SPIE, **1329**, pp. 255–265, San Diego, CA, 10–12 July 1990.
5. H. S. Judeikis, G. S. Arnold, M. Hill, R. C. Young Owl, and D. F. Hall, "Design of a Laboratory Study of Contaminant Film Darkening in Space," in *Scatter from Optical Components—Proceedings of the SPIE*, **1165**, pp. 406–423, San Diego, CA, 8–10 August 1989.
6. D. F. Hall, "Current Flight Results from the P78-2 (SCATHA) Spacecraft Contamination and Coatings Degradation Experiment," *Proceedings of the International Symposium on Spacecraft Materials in the Space Environment*, ESTEC, Noordwijk, Holland, 1982, pp. 143–148.
7. D. F. Hall, "Flight Measurement of molecular contaminant deposition," in *Optical System Contamination: Effects, Measurements, and Control IV*, Proceedings of SPIE, **2261**, 5–7 August 1996, Denver CO, pp. 58–71.
8. G. K. Ternet, J. D. Barrie and K. R. Olson, "Optical scatter from non-uniform molecular films," in *Optical Systems Degradation: Contamination, and Stray Light: Effects, Measurements and Control*, Proceedings of SPIE, **5526**, 2–5 August 2004, Denver, CO, pp. 70–78.
9. W. Krone-Schmidt and R. C. Loveridge, "Cryovacuum BRDF measurements of MMH-nitrate," in *Optical System Contamination: Effects, Measurement, Control III*, SPIE **1754**, 23–24 July 1992, San Diego CA, pp. 58–71.
10. B. L. Seiber, R. J. Bryson, W. T. Bertrand, and B. E. Wood, "Cryogenic BRDF Measurements at 10.6  $\mu\text{m}$  and 0.63  $\mu\text{m}$  on Contaminated Mirrors," AEDC-TR-94-16, Arnold Engineering Development Center, February 1995.
11. R. M. Villahermosa and D. J. Coleman, Private Communication (2003).
12. P-G deGennes, F. Brochard-Wyart, and D. Quere, "Capillarity and Wetting Phenomena: Drops, Bubbles, Pearls, Waves," Springer, New York, 2004.
13. Lawrence E. Murr, *Interfacial Phenomena in Metals and Alloys*, Addison-Wesley Publishing Co., Reading MA, 1975.

## LABORATORY OPERATIONS

The Aerospace Corporation functions as an “architect-engineer” for national security programs, specializing in advanced military space systems. The Corporation's Laboratory Operations supports the effective and timely development and operation of national security systems through scientific research and the application of advanced technology. Vital to the success of the Corporation is the technical staff's wide-ranging expertise and its ability to stay abreast of new technological developments and program support issues associated with rapidly evolving space systems. Contributing capabilities are provided by these individual organizations:

**Electronics and Photonics Laboratory:** Microelectronics, VLSI reliability, failure analysis, solid-state device physics, compound semiconductors, radiation effects, infrared and CCD detector devices, data storage and display technologies; lasers and electro-optics, solid-state laser design, micro-optics, optical communications, and fiber-optic sensors; atomic frequency standards, applied laser spectroscopy, laser chemistry, atmospheric propagation and beam control, LIDAR/LADAR remote sensing; solar cell and array testing and evaluation, battery electrochemistry, battery testing and evaluation.

**Space Materials Laboratory:** Evaluation and characterizations of new materials and processing techniques: metals, alloys, ceramics, polymers, thin films, and composites; development of advanced deposition processes; nondestructive evaluation, component failure analysis and reliability; structural mechanics, fracture mechanics, and stress corrosion; analysis and evaluation of materials at cryogenic and elevated temperatures; launch vehicle fluid mechanics, heat transfer and flight dynamics; aerothermodynamics; chemical and electric propulsion; environmental chemistry; combustion processes; space environment effects on materials, hardening and vulnerability assessment; contamination, thermal and structural control; lubrication and surface phenomena. Microelectromechanical systems (MEMS) for space applications; laser micromachining; laser-surface physical and chemical interactions; micropropulsion; micro- and nanosatellite mission analysis; intelligent microinstruments for monitoring space and launch system environments.

**Space Science Applications Laboratory:** Magnetospheric, auroral and cosmic-ray physics, wave-particle interactions, magnetospheric plasma waves; atmospheric and ionospheric physics, density and composition of the upper atmosphere, remote sensing using atmospheric radiation; solar physics, infrared astronomy, infrared signature analysis; infrared surveillance, imaging and remote sensing; multispectral and hyperspectral sensor development; data analysis and algorithm development; applications of multispectral and hyperspectral imagery to defense, civil space, commercial, and environmental missions; effects of solar activity, magnetic storms and nuclear explosions on the Earth's atmosphere, ionosphere and magnetosphere; effects of electromagnetic and particulate radiations on space systems; space instrumentation, design, fabrication and test; environmental chemistry, trace detection; atmospheric chemical reactions, atmospheric optics, light scattering, state-specific chemical reactions, and radiative signatures of missile plumes.

## LABORATORY OPERATIONS

The Aerospace Corporation functions as an "architect-engineer" for national security programs, specializing in advanced military space systems. The Corporation's Laboratory Operations supports the effective and timely development and operation of national security systems through scientific research and the application of advanced technology. Vital to the success of the Corporation is the technical staff's wide-ranging expertise and its ability to stay abreast of new technological developments and program support issues associated with rapidly evolving space systems. Contributing capabilities are provided by these individual organizations:

**Electronics and Photonics Laboratory:** Microelectronics, VLSI reliability, failure analysis, solid-state device physics, compound semiconductors, radiation effects, infrared and CCD detector devices, data storage and display technologies; lasers and electro-optics, solid-state laser design, micro-optics, optical communications, and fiber-optic sensors; atomic frequency standards, applied laser spectroscopy, laser chemistry, atmospheric propagation and beam control, LIDAR/LADAR remote sensing; solar cell and array testing and evaluation, battery electrochemistry, battery testing and evaluation.

**Space Materials Laboratory:** Evaluation and characterizations of new materials and processing techniques: metals, alloys, ceramics, polymers, thin films, and composites; development of advanced deposition processes; nondestructive evaluation, component failure analysis and reliability; structural mechanics, fracture mechanics, and stress corrosion; analysis and evaluation of materials at cryogenic and elevated temperatures; launch vehicle fluid mechanics, heat transfer and flight dynamics; aerothermodynamics; chemical and electric propulsion; environmental chemistry; combustion processes; space environment effects on materials, hardening and vulnerability assessment; contamination, thermal and structural control; lubrication and surface phenomena. Microelectromechanical systems (MEMS) for space applications; laser micromachining; laser-surface physical and chemical interactions; micropropulsion; micro- and nanosatellite mission analysis; intelligent microinstruments for monitoring space and launch system environments.

**Space Science Applications Laboratory:** Magnetospheric, auroral and cosmic-ray physics, wave-particle interactions, magnetospheric plasma waves; atmospheric and ionospheric physics, density and composition of the upper atmosphere, remote sensing using atmospheric radiation; solar physics, infrared astronomy, infrared signature analysis; infrared surveillance, imaging and remote sensing; multispectral and hyperspectral sensor development; data analysis and algorithm development; applications of multispectral and hyperspectral imagery to defense, civil space, commercial, and environmental missions; effects of solar activity, magnetic storms and nuclear explosions on the Earth's atmosphere, ionosphere and magnetosphere; effects of electromagnetic and particulate radiations on space systems; space instrumentation, design, fabrication and test; environmental chemistry, trace detection; atmospheric chemical reactions, atmospheric optics, light scattering, state-specific chemical reactions, and radiative signatures of missile plumes.



2350 E. El Segundo Boulevard  
El Segundo, California 90245-4691  
U.S.A.